Dalton Transactions

Photoinduced interactions of two dirhodium complexes with d(GTCGAC)2 probed by 2D NOESY

Journal:	*Dalton Transactions*
Manuscript ID:	DT-ART-10-2014-003119.R1
Article Type:	Paper
Date Submitted by the Author:	03-Dec-2014
Complete List of Authors:	Palmer, Alycia; The Ohio State University, Chemistry and Biochemistry Knoll, Jessica; The Ohio State University, Chemistry and Biochemistry Turro, Claudia; The Ohio State University, Department of Chemistry

Photoinduced interactions of two dirhodium complexes with d(GTCGAC)$_2$ probed by 2D NOESY

Alycia M. Palmer, Jessica D. Knoll, and Claudia Turro*

Department of Chemistry and Biochemistry, The Ohio State University, Columbus, OH 43210

Abstract. The interactions between the 6-mer duplex oligonucleotide d(GTCGAC)$_2$ and the photoactive dirhodium complexes *cis-H,H*-[Rh_2(HNOCCH$_3$)$_2$(L)(CH$_3$CN)$_4$]$^{2+}$, where L represents bpy (**1**, 2,2′-bipyridine) and dppz (**2**, dipyrido[3,2-*a*:2′,3′-*c*]phenazine), were probed using 2D ^{1}H–^{1}H NOESY NMR spectroscopy. Complex **1** does not interact with the duplex in the dark, but binds covalently to the terminal guanine following irradiation with visible light. Similar behavior was observed for **2**, but in addition to the photoinduced covalent DNA binding, the planar dppz ligand of the complex shields the terminal cytosine protons after irradiation. The results are consistent with photoinduced guanine coordination and end-capping of the duplex through π-stacking interactions with the terminal GC base pair. These data show that in the presence of the 6-mer duplex oligonucleotide, **1** and **2** exhibit photoinduced covalent binding to DNA. In addition, the π-stacking interactions of **2** with the duplex are enhanced upon irradiation.

*Author to whom correspondence should be addressed: turro.1@osu.edu

Introduction

Cisplatin, *cis*-$[Pt(NH_3)_2Cl_2]$, approved for the treatment of ovarian and testicular cancers in 1978, remains one of the most commonly used chemotherapy drugs to date.[1-5] Upon entering the cell, thermal ligand exchange occurs to form *cis*-$[Pt(NH_3)_2(OH_2)_2]^{2+}$, and this activated form of the complex covalently binds to DNA primarily at the N7 position of guanine (G).[6] The major DNA lesion of cisplatin is 1,2-GpG intrastrand crosslinks that inhibit transcription and DNA replication and trigger signal induction pathways leading to apoptosis. However, a major drawback of cisplatin is its lack of selectivity between rapidly dividing cells that are healthy and those that are cancerous.[7] In addition, acquired resistance to cisplatin requires larger doses for efficacy, which can result in severe side effects.[8] Dirhodium complexes have been previously shown to bind covalently to DNA in a manner similar to cisplatin and to exhibit antitumor activity.[9-24]

Photodynamic therapy (PDT) is a technique currently in use that circumvents the systemic toxicity associated with traditional chemotherapy drugs. The drugs used for PDT are only cytotoxic upon light activation, thus providing spatiotemporal control of the activity.[25, 26] PDT agents, such as Photofrin® (hematoporphyrin and its oligomers), undergo energy transfer to generate $^1O_2$ upon low-energy irradiation. In this and other PDT drugs, $^1O_2$ is the active species that results in damage to biomolecules and induces cell death.[27, 28] PDT is useful for endoscopically accessible tumors and is currently in use for the treatment of bladder, esophageal, head and neck, lung, prostate, gynecological, and gastrointestinal lesions.[29-33] The low O_2 concentration in many tumors, however, presents challenges in this type of light-activated cancer therapy.[34]

Transition metal complexes that covalently bind to DNA following photoinduced ligand exchange are being actively pursued to overcome the

challenges presented by both cisplatin-type chemotherapy drugs and traditional PDT agents, since their photoreactivity is independent of oxygen. For example, the dirhodium(II,II) complex *cis*-$[Rh_2(CH_3CO_2)_2(CH_3CN)_6]^{2+}$ readily exchanges the two axial CH_3CN ligands in aqueous media to generate *cis*-$[Rh_2(CH_3CO_2)_2(CH_3CN)_4(OH_2)_2]^{2+}$, where the four remaining equatorial (*eq*) acetonitrile ligands are inert to substitution in the dark. However, the complexes exchanges two *eq* CH_3CN ligands with solvent H_2O molecules upon irradiation ($\lambda > 395$ nm), and the resulting species covalently binds to DNA.[35] Ligand exchange and covalent binding do not occur in solution in the dark, and this complex exhibits a significantly greater increase in toxicity toward Hs-27 human skin fibroblasts upon irradiation compared to hematoporphyrin. The acetamide-bridged analogs *H,T*- and *H,H*-*cis*-$[Rh_2(OCCH_3NH)_2(CH_3CN)_6]^{2+}$ also exchange two *eq* CH_3CN ligands with H_2O upon irradiation and covalently bind to ds-DNA.[36] Moreover, the related complexes *cis*-*H,H*-$[Rh_2(OCCH_3NH)_2(L)(CH_3CN)_2]^{2+}$, where L = 2,2′-bipyridine (bpy, **1**) or dipyrido[3,2-*a*:2′,3′-*c*]phenazine (dppz, **2**), depicted in Figure 1, coordinate to DNA upon photoinduced CH_3CN exchange when irradiated in H_2O and, in the case of **2**, also intercalate between the base pairs of the duplex.[37] This dual activity of **2** is of interest because compounds with novel DNA binding modes, such as simultaneous intercalation and coordination, have been shown to overcome cisplatin resistance.[38,39] The light activated intercalation and covalent DNA binding with **2** provides spatiotemporal control not available with the previous dual-binding platinum compounds. However, the details on the site selectivity of the DNA binding of **2** remain unknown.

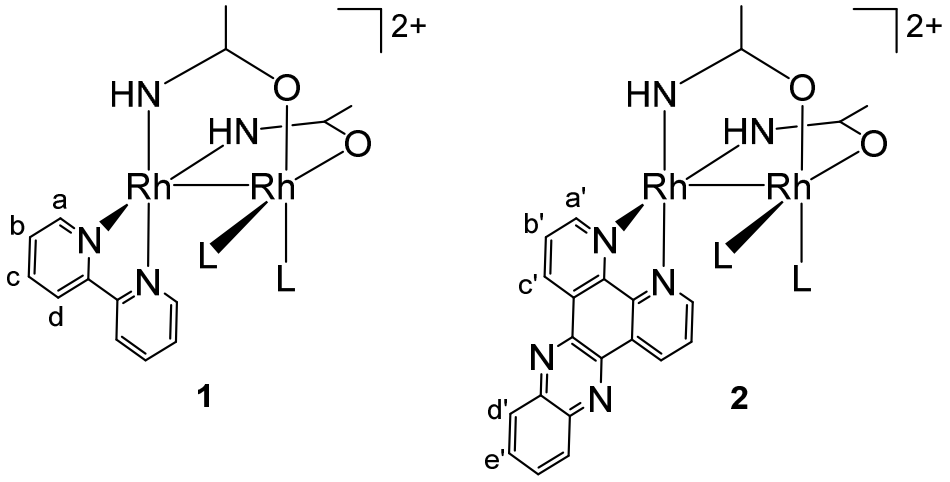

Figure 1. Structural representations and ^{1}H NMR labeling scheme of **1** and **2** (L = CH_3CN); axial ligands omitted for clarity.

The interactions between DNA and many different transition metal complexes have been probed using 2D ^{1}H–^{1}H Nuclear Overhauser Effect Spectroscopy (NOESY). A notable example is the binding of cisplatin to the GG step of d(5′-TCTCGGTCTC-3′) annealed with its complementary strand, resulting in a 1,2-intrastrand *cis*-[$Pt(NH_3)_2${d(GpG)}] crosslink.[40] A dinuclear compound, [(*cis*-{$Pt(NH_3)_2$})$_2$(μ-OH)(μ-pz)]$^{2+}$ (pz = pyrazole bridging ligand) forms a GpG intrastrand crosslink with d(5′-CTCTG*G*TCTC-3′)•d(5′-GAGACCAGAG-3′) (asterisks indicate location of metal binding); the binding of the complexes decreases the H1′-H1′ distance in the GpG step without a significant bend in the duplex's helical axis compared to the unplatinated duplex.[41] Similarly, when [$Rh_2(O_2CCH_3)_4$] and single-stranded d(5′-CTCTCAACTTCC-3′) were incubated at 37 ^{o}C for 4-5 h, then annealed with the complementary strand, the downfield shifts by 0.4 – 0.6 ppm of the C_5 and A_6 signals were attributed to the formation of a 1,2-intrastrand adduct between these two nucleobases.[24] In an analogous experiment with *cis*-[Rh_2(dap)(μ-O_2CCH_3)(η^1-O_2CCH_3)(CH_3OH)]$^{+}$ (dap = 1,12-

diazaperylene), it was shown that the dap ligand intercalates between the A_6 and A_7 bases, as evidenced by a 0.12 ppm upfield shift of the dap resonances and the through-space coupling of dap protons with H2 and H8 of A_6 and A_7 of the duplex. Additionally, covalent binding occurs at the N7 position of A_6, which appears as a downfield shift of the A_6H8 signal by 0.14 ppm.[42] This complex represents the first dirhodium(II,II) complex that exhibits dual DNA binding through intercalation and covalent adduct formation.

2D ^{1}H NMR measurements were also used to demonstrate the enantioselective intercalation of Ru(II) complexes featuring the dppz ligand with the palindromic d(5′-GTCGAC-3′)$_2$ duplex, where an NOE signal was detected between the deoxyribose H2′ and H2″ and the proximal dppz protons in Δ-$[Ru(phen)_2(dppz)]^{2+}$ (phen = 1,10-phenanthroline).[43-46] In the case of Δ-$[Ru(Me_2phen)_2(dppz)]^{2+}$ (Me_2phen = 4,7-dimethyl-1,10-phenanthroline), NMR data indicates that the complex was intercalates between the G_4–C_3 and A_5–T_2 base pairs from the minor groove.[47] In the mismatched sequence d(5′-CGGAAATTACCG-3′)$_2$ (mismatched bases are underlined), $[Ru(bpy)_2(dppz)]^{2+}$ was co-crystallized with the oligonucleotide, demonstrating metalloinsertion at the mismatch site, intercalation at well-matched sites, and an end-capping interaction; the latter is characterized by π-stacking of the dppz ligand with the last set of paired bases in the duplex.[48]

In the present work, the photoinduced binding of complexes **1** and **2** to a duplex 6-mer oligonucleotide formed by the annealing of the palindromic sequence 5′-GTCGAC-3′, d(GTCGAC)$_2$, was investigated. Previous work showed that both complexes undergo photoinduced covalent binding to the 12-mer duplex oligonucleotide d(5′-CTCTCAACTTCC-3′)•d(5′-GGAAGTTGAGAG-3′), but **2** also exhibits enhanced intercalation following irradiation.[37] To elucidate the specific binding sites of **1** and **2**, 2D ^{1}H–^{1}H

NOESY and thermal denaturation experiments were conducted with the shorter d(GTCGAC)$_2$ duplex both in the dark and upon irradiation with visible light.

Experimental

Materials. Complexes **1** and **2** were synthesized as previously reported.[37] The 6-mer DNA was purchased from the Midland Certified Reagent Company where it was purified by gel filtration chromatography prior to delivery. D_2O, K_2HPO_4, and NaCl were purchased from Sigma.

Instrumentation. NOESY experiments were performed on a Bruker 600 MHz NMR spectrometer with a triple resonance inverse cryoprobe. Samples were irradiated using a 450 W Xe arc lamp (OSRAM Sylvania XBO) in an A6000 lamp housing (PTI) powered by an LPS-500 power supply (PTI). Electronic absorption spectra were obtained with a Hewlett-Packard 8453 diode array spectrophotometer equipped with a digitally controlled HP 89090A Peltier temperature controller and UV-Vis ChemStation software in Thermal Denaturation mode.

Methods. The oligonucleotide concentration was determined by electronic absorption spectroscopy using the molar absorptivity provided by the vendor and confirmed by the known molar extinction coefficient of each nucleotide (260 nm, ε = 62,100 $M^{-1}cm^{-1}$ per single strand).[49]

NOESY experiments were run at 16 °C, collecting 1024 points along F2 and 512 t_1 blocks with 32 scans per block. Water suppression was performed by presaturation during relaxation delay, and the mixing time was set to 280 ms. Data collection for one NOESY experiment occurred over 8 h. Samples were prepared by dissolving a known amount of 6-mer DNA in 10 mM sodium phosphate buffer (pH = 7) with 20 mM NaCl and 0.2 mM DSS (sodium-2,2-dimethyl-2-silapentane-5-sulfonate). To anneal the DNA, the solution containing

200 μM single stranded oligonucleotide was heated to 90 °C in the same buffer, then allowed to slowly cool to room temperature in the heat block. The annealed sample was lyophilized in D_2O and then reconstituted with 99.998% D_2O to give 310 μL of 1.6 mM duplex 6-mer. The solution was combined with a portion of a stock solution of the corresponding complex to attain 1:1 and 1:0.75 [duplex]:[complex] for **1** and **2**, respectively, allowed to mix at room temperature for 1 hr, and the final complex concentration was ascertained by electronic absorption spectroscopy. Each solution was transferred to a Shigemi tube for the NMR experiment and precautions were taken to protect it from room light.

Each sample was first used for the dark NMR experiment and after remaining in solution in the dark at room temperature for up to 1 day, it was then irradiated for 6 h with $\lambda \geq 395$ nm using a glass long-pass filter (CVI Melles Griot), and the sample holder was submerged in a circulating water bath to maintain constant temperature and absorb infrared light produced by the lamp. The sample was then purified to remove free complex using an Amicon Pro 3k centrifuge filter. The column was first centrifugated for 30 minutes at 13,093 rpm in a Cole Parmer (3400 rpm) centrifuge. The column was then inverted into a second vial and centrifugated for 10 minutes at 3,500 rpm to collect the concentrated, purified product. The liquid was reconstituted with buffer to maintain the 310 μL volume, and then lyophilized to remove H_2O. Finally, the purified sample was dissolved in D_2O for analysis by NMR. Chemical shift values are a result of two experiments averaged, and error bars depict the average error.

The samples for the dark thermal denaturation experiments were prepared by adding 70 μL of 300 μM metal complex in phosphate buffer (40 mM K_2HPO_4, 300 mM NaCl, pH = 6.89) to 3.36 mL of the same phosphate buffer solution in a 1 × 1 cm quartz cuvette. A 70 μL sample of 200 μM duplex was added to the cuvette (final volume = 3.5 mL) to give final concentrations of 6 μM metal

complex and 4 μM duplex, and the sample was incubated at room temperature in the dark for 1 h. For the irradiated experiments, 70 μL of 200 μM duplex and 70 μL of 300 μM metal complex were combined and diluted to 500 μL. The solution was irradiated with $\lambda_{irr} \geq 395$ nm for 3 h and was then diluted to 3.5 mL with phosphate buffer to give the same concentrations as those used in the corresponding dark experiments. The temperature was set to increase from 16 °C to 55 °C in increments of 1 °C using the Peltier temperature controller. At each temperature, a one minute hold time was applied to equilibrate the temperature prior to measuring the absorbance of the duplex at 260 nm. The data, plotted as the absorbance at 260 nm vs temperature, were fit to a Boltzmann sigmoidal curve using OriginPro 8. Each melting temperature value (T_m) given is the point of inflection of the curve as reported by the software.

Results and Discussion

$^1H-^1H$ NOESY experiments were performed with the 6-mer $d(GTCGAC)_2$ duplex to obtain structural information about the specific binding sites of **1** and **2** both in the dark and upon irradiation with visible light. The chemical shifts of the bpy and dppz ligand protons of **1** and **2**, respectively, were compared in the presence and absence of the duplex, and the results are listed in Table 1. After the addition of 0.75 equivalents of duplex $d(GTCGAC)_2$, the dppz proton resonances of **2** shift upfield between +0.11 and +0.29 ppm, which is consistent with shielding due to close proximity of the π-system of a nucleobase. In contrast, the change in chemical shifts, Δδ, for the bpy ligand in **1** in the presence of the 6-mer was only between +0.02 and +0.06 ppm, inconsistent with shielding of the bpy protons by duplex since these values are within experimental error ($\Delta\delta = \pm 0.06$ ppm). These data show that the dppz ligand of **2** is involved in π-stacking with DNA nucleobases, but that the interaction with the bpy ligand of complex **1** is not

significant. It should be noted that after irradiation with $\lambda_{irr} \geq 395$ nm, the ligand proton resonances were not well resolved when DNA was present, such that definitive assignments were not possible. The inability to assign the dppz photons after irradiation can be ascribed to the reduced symmetry of the molecule upon photoinduced exchange of only one equatorial CH_3CN for a solvent D_2O molecule.

Table 1. Chemical shifts of ligand protons on **1** and **2** in the absence and presence of $d(GTCGAC)_2$ in the dark (see labelling scheme in Figure 1).

		δ /ppm		
Complex	Proton	no DNA [a]	with DNA [a,b]	Δδ / ppm
1	a	8.88	8.94	0.06
	b	7.74	7.76	0.02
	c	8.20	8.24	0.04
	d	8.47	8.52	0.05
2	a′	9.76	9.47	-0.29
	b′	8.28	8.12	-0.16
	c′	9.37	9.26	-0.11
	d′	8.43	8.14	-0.29
	e′	8.12	7.96	-0.16

[a] In 10 mM sodium phosphate buffer (pH = 7) and 20 mM NaCl. [b] 1:1 [**1**]:[duplex] or 0.75:1.00 [**2**]:[duplex]

The changes in the chemical shifts of the 6-mer duplex protons upon addition of metal complex were also measured to provide information on the binding of each complex. Chemical shifts for the protons of the 6-mer duplex in the absence of a metal complex were previously reported.[43] The chemical shift was determined for each DNA proton in the presence of 0.75 equivalents of **2** in the dark and after irradiation for 6 hours ($\lambda_{irr} \geq 395$ nm) and are reported in Table 2.

The difference plot in Figure 2 shows the average value of Δδ, where Δδ = δ(irradiated) – δ(dark), for selected proton resonances in the 6-mer sequence. A positive value of Δδ reflects a downfield shift, and a negative value reflects an upfield shift; the numbering scheme of the base pairs is shown in the inset of Figure 2. The difference plot highlights two main interactions that occur upon irradiation. Namely, the G_1H8 protons shift significantly downfield from 7.90 to 8.23 ppm after irradiation (Δδ = +0.33 ppm) and the C_6H6 protons shift upfield from 7.30 to 7.03 ppm after irradiation (Δδ = −0.27 ppm).

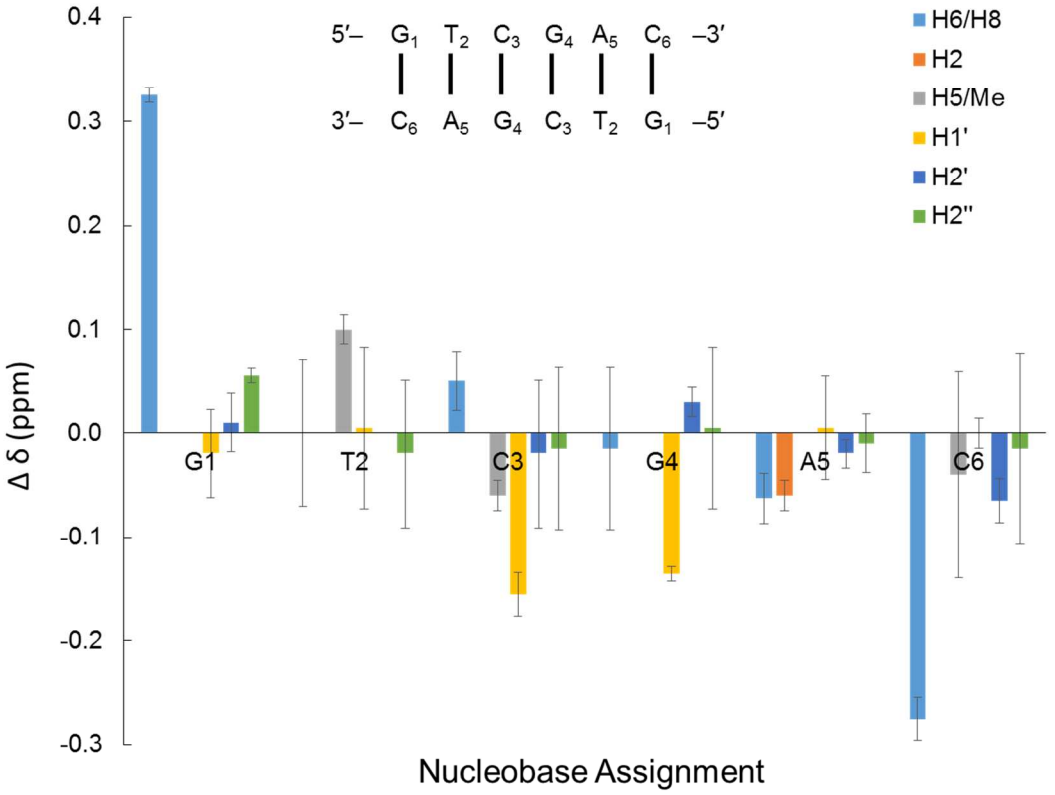

Figure 2. Difference plot showing the change in chemical shift of DNA protons in the presence of **2** irradiated ($\lambda_{irr} \geq 395$ nm, 6 h) relative to the dark, where Δδ = δ(irradiated) – δ(dark). The inset shows the numbering scheme for the duplex $d(GTCGAC)_2$.

Table 2. Chemical shifts of DNA protons for d(GTCGAC)$_2$ in the presence of 0.75 equivalents of **2** in the dark and after irradiation ($\lambda > 395$ nm).

		δ (ppm)				
Base	**Proton**	**DNA Only**[a]	**Dark**[b]	**Irradiated**[b,c]	**Δδ**	**Error**
	H8	7.98	7.90	8.23	0.33	0.01
G_1	H1′	6.02	5.99	5.97	-0.02	0.04
	H2′	2.82	2.79	2.81	0.02	0.03
	H2″	2.73	2.63	2.69	0.06	0.01
	H6	7.53	7.44	7.44	0.00	0.07
	Me	1.34	1.21	1.31	0.10	0.01
T_2	H1′	6.19	6.09	6.15	0.06	0.08
	H2′	2.25	2.22	2.22	0.00	0.01
	H2″	2.59	2.54	2.52	-0.02	0.07
	H6	7.50	7.44	7.46	0.02	0.03
	H5	5.67	5.62	5.56	-0.06	0.01
C_3	H1′	5.68	5.62	5.46	-0.16	0.02
	H2′	2.06	2.02	2.00	-0.02	0.07
	H2″	2.42	2.37	2.36	-0.02	0.08
	H8	7.96	7.92	7.91	-0.02	0.08
G_4	H1′	5.61	5.55	5.42	-0.14	0.01
	H2′	2.80	2.75	2.78	0.03	0.01
	H2″	2.75	2.70	2.71	0.01	0.08
	H8	8.18	8.15	8.09	-0.06	0.02
	H2	7.97	7.93	7.87	-0.06	0.01
A_5	H1′	6.28	6.22	6.22	0.01	0.05
	H2′	2.65	2.64	2.62	-0.02	0.01
	H2″	2.91	2.89	2.88	-0.01	0.03
	H6	7.30	7.30	7.03	-0.27	0.02
	H5	5.28	5.21	5.17	-0.04	0.10
C_6	H1′	6.04	5.99	5.99	0.00	0.01
	H2′	2.11	2.18	2.11	-0.07	0.02
	H2″	2.11	2.18	2.11	-0.07	0.09

[a] Determined for 1.4 mM d(GTCGAC)$_2$ in 10 mM sodium phosphate buffer (pH = 7.0) with 20 mM NaCl. Referenced to internal DSS. Assignments were based on those reported in reference.

[b] Values are averaged over two datasets acquired under identical conditions.

[c] Irradiation with $\lambda_{irr} \geq 395$ nm, 6 h. When more than one shift was observed, the largest shift was reported.

The shift of the resonance associated with G_1H8 is displayed in Figure 3. The T_2Me/G_1H8 correlation under dark conditions (Figure 3a) splits into two NOE signals after irradiation (Figure 3b), where the new cross peak is labelled T_2'Me/G_1'H8. The T_2Me/G_1H8 signal corresponds to the resonance of the unmodified base, while the T_2′Me/G_1′H8 signal is shifted downfield and corresponds to the resonance of the metallated site. Two signals are observed because there are two G_1 nucleobases per duplex, but only 0.75 equivalents of complex to duplex are present. Therefore, only one of the two G_1 sites is expected to be associated with the complex on average.

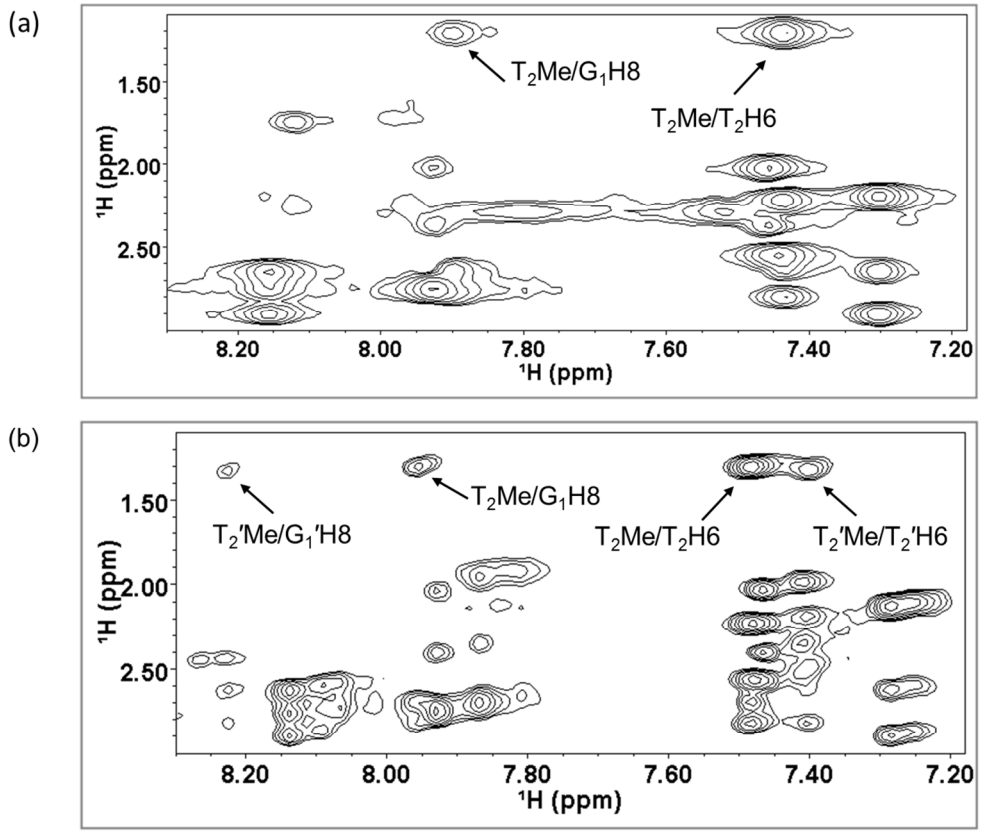

Figure 3. NOESY spectrum of d(GTCGAC)$_2$ with **2** (a) in the dark and (b) after irradiation (($\lambda_{irr} \geq$ 395 nm, 6 h).

The correlation of the methyl and H6 protons on T_2 (T_2Me/T_2H6) only shifts slightly after irradiation, T_2'Me/T_2'H6 (Figure 3). This small shift indicates that the dppz ligand is not intercalated between the G_1–C_6 and T_2–A_5 base pairs, since a greater effect on the position of the T_2H6 resonance would be expected upon intercalation at that step. Therefore, the large upfield shift of C_6H6 is indicative that the dppz ligand of **2** is π-stacking with the terminal GC base pairs only as an end-capping interaction with the duplex. The NOESY spectra depicting the shift of the C_6H6 resonance after irradiation is shown in Figure S1. A similar end-capping π-stacking interaction was also reported in the crystal structure of $[Ru(bpy)_2(dppz)]^{2+}$ with a duplex oligonucleotide.[48] The observed $\Delta\delta$ = +0.33 ppm for G_1H8 in **2** is smaller than the $\Delta\delta$ = +0.55 ppm measured for $Rh_2(O_2CCH_3)_4$, which covalently binds to A_6 in d(CTCTCAACTTCC)• d(GGAAGTTGAGAG).[24] The positive $\Delta\delta$ values are associated with deshielding of the nucleobase protons upon covalent binding by a transition metal. Although Rh-coordination to A or G by **2** and $Rh_2(O_2CCH_3)_4$ are expected exhibit a similar shift, in the case of complex **2**, there is also the shielding effect of π-stacking by aromatic ligands, thus diminishing the overall deshielding effect imparted by the covalent binding. Therefore, the resulting shift is a combination of both effects, leading to a smaller value of $\Delta\delta$ relative to metal coordination alone. This trend was also apparent in the $\Delta\delta$ = +0.14 ppm value reported for *cis*-$[Rh_2(dap)(\mu\text{-}O_2CCH_3)(\eta^1\text{-}O_2CCH_3)(CH_3OH)]^+$ that covalently binds at the A_6 position of d(CTCTCAACTTCC)•d(GGAAGTTGAGAG) while also intercalating between the A_6 and A_7 nucleotides.[42]

To confirm that the upfield shift of the C_6H6 resonance was due to a π-stacking interaction with the dppz ligand of **2**, the experiment was repeated with complex **1**, which contains the smaller, non-intercalating bpy ligand. The difference plot showing the changes in the chemical shifts following irradiation

of **1** with d(GTCGAC)$_2$ are presented in Figure 4. Similar to **2**, the G_1H8 proton resonance shifts downfield from 7.98 to 8.19 ppm ($\Delta\delta$ = +0.21 ppm) upon irradiation. The C_6H6 proton resonance also shifts downfield, though to a smaller extent, from 7.29 to 7.41 ppm ($\Delta\delta$ = +0.12 ppm). Table 3 list the chemical shifts and $\Delta\delta$ values for each proton, and the NOESY spectra showing the G_1H8 and C_6H6 resonances in the dark and after irradiation are shown in Figures S2 and S3, respectively. Since upfield shifting of the C_6H8 proton resonance is only observed with **2** and not **1**, the upfield shift upon irradiation of the mixture with **2** is attributed to increased shielding by the dppz ligand.

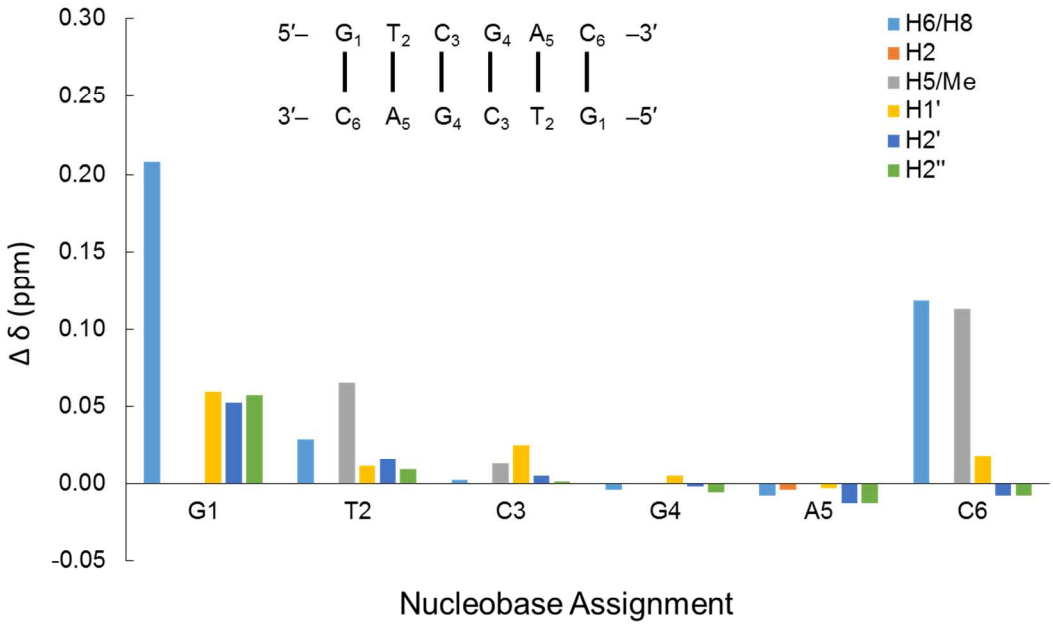

Figure 4. Difference plot showing the change in chemical shift of DNA protons in the presence of **1** irradiated ($\lambda_{irr} \geq 395$ nm) relative to the dark, where $\Delta\delta$ = δ(irradiated) – δ(dark). The inset shows the numbering scheme for the duplex d(GTCGAC)$_2$.

Table 3. Chemical shifts of DNA protons for d(GTCGAC)$_2$ in the presence of 1.0 equivalent of **1** in the dark and after irradiation ($\lambda_{irr} \geq 395$ nm).

		δ (ppm)			
Base	**Proton**	**DNA Only**[a]	**Dark**[b]	**Irradiated**[b,c]	**Δδ**
	H8	7.98	7.98	8.19	0.21
G_1	H1′	6.02	5.96	6.02	0.06
	H2′	2.82	2.76	2.81	0.06
	H2″	2.73	2.67	2.73	0.06
	H6	7.53	7.50	7.53	0.03
	Me	1.34	1.25	1.31	0.07
T_2	H1′	6.19	6.19	6.20	0.01
	H2′	2.25	2.23	2.25	0.02
	H2″	2.59	2.58	2.59	0.01
	H6	7.50	7.50	7.50	0.00
	H5	5.67	5.68	5.69	0.01
C_3	H1′	5.68	5.66	5.67	0.03
	H2′	2.06	2.05	2.06	0.01
	H2″	2.42	2.43	2.43	0.00
	H8	7.96	7.98	7.97	0.00
G_4	H1′	5.61	5.62	5.62	0.01
	H2′	2.80	2.81	5.81	0.00
	H2″	2.75	2.76	2.75	-0.01
	H8	8.18	8.20	8.19	-0.01
	H2	7.97	7.98	7.97	0.00
A_5	H1′	6.28	6.29	6.29	0.00
	H2′	2.65	2.65	2.65	-0.01
	H2″	2.91	2.93	2.92	-0.01
	H6	7.30	7.29	7.41	0.12
	H5	5.28	5.28	5.39	0.11
C_6	H1′	6.04	6.03	6.04	0.02
	H2′	2.11	2.10	2.09	-0.01
	H2″	2.11	2.10	2.09	-0.01

[a] Determined for 1.4 mM d(GTCGAC)$_2$ in 10 mM sodium phosphate buffer (pH = 7.0) with 20 mM NaCl. Referenced to internal DSS. Assignments were based on those reported in reference.
[b] Mixture contains 1.6 mM d(GTCGAC)$_2$ in 10 mM sodium phosphate buffer (pH = 7.0) with 20 mM NaCl.
[c] Irradiation with $\lambda_{irr} \geq$ 395 nm, 6 h. When more than one shift was observed, the largest shift is reported.

Thermal denaturation experiments support the proposed interactions between the duplex and the metal complexes as determined by ^{1}H–^{1}H NOESY. The

melting temperatures (T_m) of d(GTCGAC)$_2$ alone and in the presence of each complex under both dark and irradiated conditions are provided in Table 2. A slight increase in T_m of the duplex, ΔT_m = +0.7 °C, was observed in the presence of **2**, consistent with the proposed weak interaction between duplex and the complex when the dppz ligand π-stacks in and end-capping fashion to the duplex. Upon irradiation with $\lambda_{irr} \geq$ 395 nm for 3 h, the complex covalently binds to the duplex, providing a stronger end-capping interaction and reducing fraying, resulting in a larger ΔT_m value, +4.8 °C. Analogous experiments with **1** result in no substantial impact on T_m in the dark, but slightly greater destabilization following irradiation, consistent with the lack of π-stacking interactions between the complex and the base pairs and the covalent binding at the terminal G_1 nucleobase upon irradiation.

Table 4. Thermal denaturation of d(GTCGAC)$_2$ in the absence and presence of **1** and **2** in the dark and irradiated.

Complex [a]	T_m^{Dark} / °C	ΔT_m^{Dark} / °C	T_m^{Irr} / °C [b]	ΔT_m^{Irr} / °C
None	30.9(6)		*c*	*c*
1	30.5(6)	–0.4	29.6(8)	–1.3
2	31.6(5)	+0.7	35.7(4)	+4.8

[a] In 40 mM sodium phosphate buffer and 300 mM NaCl (pH = 6.89). Samples contained 4 μM duplex and 0 or 6 μM complex.
[b] Samples were irradiated for 3 h with λ > 395 nm.
[c] Not measured

Conclusions

The NOESY data show that both **1** and **2** undergo photoinduced covalent binding to the terminal guanine nucleobase of the 6-mer duplex oligonucleotide d(GTCGAC)**$_2$** based on downfield shifts of the G_1H8 resonances upon irradiation. In the dark, a weak π-stacking and electrostatic interaction is present between **2**

and the duplex due to the dppz ligand and the overall positive charge of the complex. Upon photodissociation of one CH_3CN ligand, the metal complex covalently binds to the N7 of G_1, providing a stronger π-stacking interaction of the distal portion of dppz with the terminal bases in an end-capping fashion. The data are also consistent with covalent binding of **1** with G_1, with no π-stacking interactions with the nucleobases. Thermal denaturation experiments confirm stabilization of the duplex upon irradiation with **2** and not **1**, and this is consistent with the proposed binding modes. Intercalation of dppz in **2** between base pairs rather than end-capping is expected to occur in native DNA, so NOESY experiments are underway to analyze the interactions of **1** and **2** with longer oligonucleotide sequences.

Acknowledgements

The authors would like to thank Dr. Chunhua Yuan for assistance with NMR methods. We also thank the National Institutes of Health (1RO1 EB016072) and National Science Foundation (CHE-1213646) for partial support of this work.

Notes

Electronic Supplementary Information (ESI) available: Additional NOESY spectra and tables of chemical shifts. See DOI: 10.1039/b000000x/

References

1. B. Rosenberg, *Interdiscipl. Sci. Rev.*, 1978, **3**, 134-147.

2. B. Rosenberg, L. Van Camp and T. Krigas, *Nature*, 1965, **205**, 698-699.

3. B. Rosenberg, L. Vancamp, J. E. Trosko and V. H. Mansour, *Nature*, 1969, **222**, 385-386.

4. E. R. Jamieson and S. J. Lippard, *Chem. Rev.*, 1999, **99**, 2467-2498.

5. K. S. Lovejoy and S. J. Lippard, *Dalton Trans.*, 2009, 10651-10659.

6. R. B. Martin, *Cisplatin*, 1999, pp. 111-134.

7. M. A. Fuertes, C. Alonso and J. M. Pérez, *Chem. Rev.* , 2003, **103**, 645-662.

8. Z. H. Siddik, *Oncogene*, 2003, **22**, 7265-7279.

9. J. D. Aguirre, A. M. Angeles-Boza, A. Chouai, J.-P. Pellois, C. Turro and K. R. Dunbar, *J. Am. Chem. Soc.*, 2009, **131**, 11353-11360.

10. J. D. Aguirre, A. M. Angeles-Boza, A. Chouai, C. Turro, J.-P. Pellois and K. R. Dunbar, *Dalton Trans.*, 2009, 10806-10812.

11. J. D. Aguirre, D. A. Lutterman, A. M. Angeles-Boza, K. R. Dunbar and C. Turro, *Inorg. Chem.*, 2007, **46**, 7494-7502.

12. A. M. Angeles-Boza, H. T. Chifotides, J. D. Aguirre, A. Chouai, P. K. L. Fu, K. R. Dunbar and C. Turro, *J. Med. Chem.*, 2006, **49**, 6841-6847.

13. H. T. Chifotides and K. R. Dunbar, *Chem. Eur. J.*, 2006, **12**, 6458-6468.

14. H. T. Chifotides and K. R. Dunbar, *J. Am. Chem. Soc.*, 2007, **129**, 12480-12490.

15. H. T. Chifotides and K. R. Dunbar, *Chem. Eur. J.*, 2008, **14**, 9902-9913.

16. H. T. Chifotides, P. K. L. Fu, K. R. Dunbar and C. Turro, *Inorg. Chem.*, 2004, **43**, 1175-1183.

17. H. T. Chifotides, J. M. Koomen, M. J. Kang, S. E. Tichy, K. R. Dunbar and D. H. Russell, *Inorg. Chem.*, 2004, **43**, 6177-6187.

18. H. T. Chifotides, K. M. Koshlap, L. M. Perez and K. R. Dunbar, *J. Am. Chem. Soc.*, 2003, **125**, 10703-10713.

19. H. T. Chifotides, K. M. Koshlap, L. M. Perez and K. R. Dunbar, *J. Am. Chem. Soc.*, 2003, **125**, 10714-10724.

20. D. V. Deubel and H. T. Chifotides, *Chem. Commun.*, 2007, 3438-3440.

21. S. U. Dunham, H. T. Chifotides, S. Mikulski, A. E. Burr and K. R. Dunbar, *Biochem.*, 2005, **44**, 996-1003.

22. A. Erck, L. Rainen, Whileyma.J, I. M. Chang, A. P. Kimball and J. Bear, *Proc. Soc. Exp. Biol. Med.*, 1974, **145**, 1278-1283.

23. R. A. Howard, A. P. Kimball and J. L. Bear, *Cancer Res.*, 1979, **39**, 2568-2573.

24. M. Kang, H. T. Chifotides and K. R. Dunbar, *Biochem.*, 2008, **47**, 2265-2276.

25. Á. Juarranz, P. Jaén, F. Sanz-Rodríguez, J. Cuevas and S. González, *Clin. Transl. Oncol.*, 2008, **10**, 148-154.

26. I. J. Macdonald and T. J. Dougherty, *J. Porphyrins Phthalocyanines*, 2001, **5**, 105-129.

27. K. Moghissi, K. Dixon, M. Stringer and J. Thorpe, *Photodiagn. Photodyn. Ther.*, 2009, **6**, 159-166.

28. C. Tanielian, C. Schweitzer, R. Mechin and C. Wolff, *Free Radical Biol. Med.*, 2001, **30**, 208-212.

29. M.-F. Zuluaga and N. Lange, *Curr. Med. Chem.*, 2008, **15**, 1655-1673.

30. R. Allison, R. Cuenca, G. Downie, P. Camnitz, B. Brodish and C. Sibata, *Photodiang. Photodyn. Ther.*, 2005, **2**, 205-222.

31. R. Allison, K. Moghissi, G. Downie and K. Dixon, *Photodiagn. Photodyn. Ther.*, 2011, **8**, 231-239.

32. P. Babilas, S. Schreml, M. Landthaler and R. M. Szeimies, *Photodermatol. Photoimmunol. Photomed.*, 2010, **26**, 118-132.

33. A. K. D'Cruz, M. H. Robinson and M. A. Biel, *Head & Neck*, 2004, **26**, 232-240.

34. L. Wyld, M. W. Reed and N. J. Brown, *Brit. J. Cancer*, 1998, **77**, 1621-1627.

35. D. A. Lutterman, P. K. L. Fu and C. Turro, *J. Am. Chem. Soc.*, 2005, **128**, 738-739.

36. S. J. Burya, A. M. Palmer, J. C. Gallucci and C. Turro, *Inorg. Chem.*, 2012, **51**, 11882-11890.

37. A. M. Palmer, S. J. Burya, J. C. Gallucci and C. Turro, *ChemMedChem*, 2014, **9**, 1260-1265.

38. G. Momekov, A. Bakalova and M. Karaivanova, *Curr. Med. Chem.*, 2005, **12**, 2177-2191.

39. Z. Ma, J. R. Choudhury, M. W. Wright, C. S. Day, G. Saluta, G. L. Kucera and U. Bierbach, *J. Med. Chem.*, 2008, **51**, 7574-7580.

40. J. H. den Hartog, C. Altona, J. H. van Boom, G. A. van der Marel, C. A. Haasnoot and J. Reedijk, *J. Biomol. Struct. Dyn.*, 1985, **2**, 1137-1155.

41. S. Teletchéa, S. Komeda, J.-M. Teuben, M.-A. Elizondo-Riojas, J. Reedijk and J. Kozelka, *Chem. Eur. J.*, 2006, **12**, 3741-3753.

42. M. Kang, A. Chouai, H. T. Chifotides and K. R. Dunbar, *Angew. Chem. Int. Ed.*, 2006, **45**, 6148-6151.

43. C. M. Dupureur and J. K. Barton, *Inorg. Chem.*, 1997, **36**, 33-43.

44. I. Haq, P. Lincoln, D. Suh, B. Norden, B. Z. Chowdhry and J. B. Chaires, *J. Am. Chem. Soc.*, 1995, **117**, 4788-4796.

45. J. P. Hall, D. Cook, S. R. Morte, P. McIntyre, K. Buchner, H. Beer, D. J. Cardin, J. A. Brazier, G. Winter and J. M. Kelly, *J. Am. Chem. Soc.*, 2013, **135**, 12652-12659.

46. H. Niyazi, J. P. Hall, K. O'Sullivan, G. Winter, T. Sorensen, J. M. Kelly and C. J. Cardin, *Nat. Chem.*, 2012, **4**, 621-628.

47. A. Greguric, I. D. Greguric, T. W. Hambley, J. R. Aldrich-Wright and J. G. Collins, *J. Chem. Soc., Dalton Trans.*, 2002, 849-855.

48. H. Song, J. T. Kaiser and J. K. Barton, *Nat. Chem.*, 2012, **4**, 615-620.

49. A. V. Tataurov, Y. You and R. Owczarzy, *Biophys. Chem.*, 2008, **133**, 66-70.

Table of Contents

2D ^{1}H-^{1}H NOESY reveals that irradiation of *cis-H,H*-[$Rh_2(HNOCCH_3)_2(dppz)(CH_3CN)_4]^{2+}$ results in covalent binding and end-capping of the complex to $d(GTCGAC)_2$.